

First results on properties and concentrations of radiation defect centers in nitrogen-enriched, high-resistivity silicon

Paweł Kamiński^a, Roman Kozłowski^a, Barbara Surma^a, and Eduardo Cortina^b

^a Institute of Electronic Materials Technology
ul. Wólczyńska 133, 01-919 Warszawa, Poland

^b Université Catholique de Louvain,
Chemin du Cyclotron 2, B-1348 Louvain-la-Neuve, Belgium

Outline

- N-doped, high-purity, high-resistivity FZ Si Samples
- Neutron irradiations
- Details of High-Resolution Photoinduced Transient Spectroscopy (HRPITS) measurements
- Properties and concentrations of electrically active irradiation-induced defect centers
- Conclusions

FZ Si nitrogen-doped, high-resistivity samples

Sample label	Oriental-tion	ρ (300 K) (Ωcm)	[N] ($\times 10^{15} \text{ cm}^{-3}$)	[O] ($\times 10^{16} \text{ cm}^{-3}$)	[C] ($\times 10^{15} \text{ cm}^{-3}$)
A (2.1)	<100>	4700	0.98	0.6	1.0
B (1.1)	<111>	1700	2.26	1.1	1.0
C (4.2)	<100>	500	1.42	< 1	< 1
D (6.1)	<100>	4100	2.0	0.5	< 1
E (8.1)	<100>	5300	0.92	0.2	< 1
F(10.2)	<111>	1700	2.5	0.9	3.0

Neutron irradiations

- ❑ Neutron irradiation facilities at Université Catholique de Louvain, Louvain-la-Neuve.
- ❑ Neutrons energy: 23 MeV.
- ❑ Three neutron fluences equivalent to the damage made by 1-MeV neutrons: 1×10^{14} , 5×10^{14} and $\sim 1 \times 10^{15} \text{ cm}^{-2}$.
- ❑ The irradiation resulted in substantial increase of the material resistivity.

Samples properties after irradiations

Sample label	Fluence (n_{eq}/cm^2)	ρ (300 K) (Ωcm)	E_{TDDC} (meV)	$[V_2^0]$
A (2.1)	1×10^{14}	1.9×10^5	334	$< 10^{12}$
B (1.1)	1×10^{14}	2.0×10^5	385	3.1×10^{12}
C (4.2)	5×10^{14}	1.4×10^4	362	1.30×10^{13}
D (6.1)	5×10^{14}	1.3×10^5	436	8.1×10^{12}
E (8.1)	1×10^{15}	1.7×10^5	426	2.8×10^{13}
F(10.2)	1×10^{15}	7.2×10^4	305	2.3×10^{13}

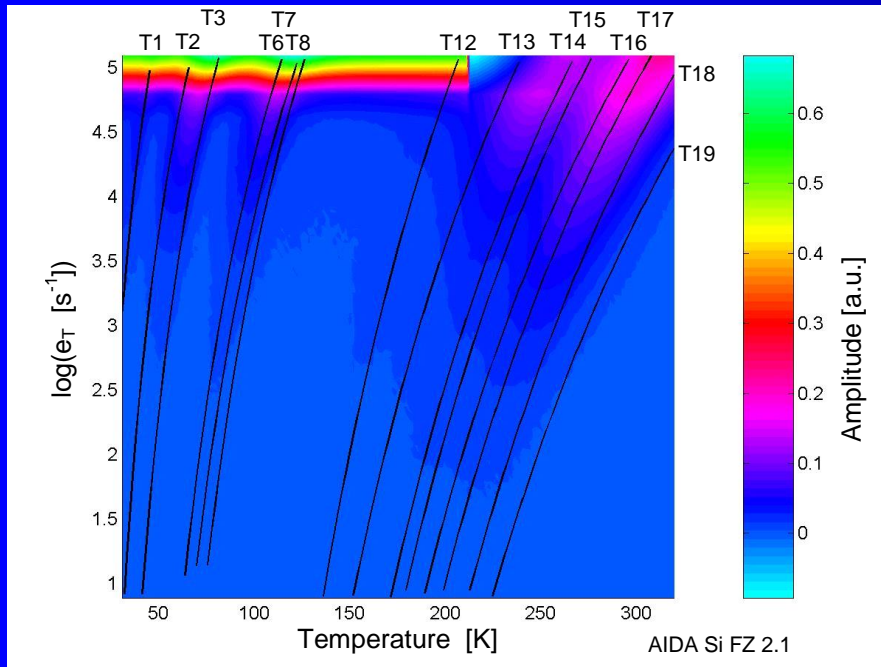
Details of HRPITS measurements

- Temperature range: 30 – 300 K, $\Delta T = 2 \text{ K}$
- Excitation source: 1 mW, 650 nm laser diode ($h\nu = 1.908 \text{ eV}$)
- Excitation pulse parameters: Width – 5 ms, Period – 500 ms
- Photon flux: $1.3 \times 10^{17} \text{ cm}^{-2}\text{s}^{-1}$
- BIAS: 20 V
- Gain: 1×10^6 – $1 \times 10^8 \text{ V/A}$
- AVG: 250 waveforms
- Analysis of photocurrent relaxation waveforms:
 - 2D inverse Laplace transformation algorithm → images of Laplace fringes for radiation defect centers
 - 2D correlation procedure (multi-window approach) → images of correlation spectral fringes for radiation defect centers

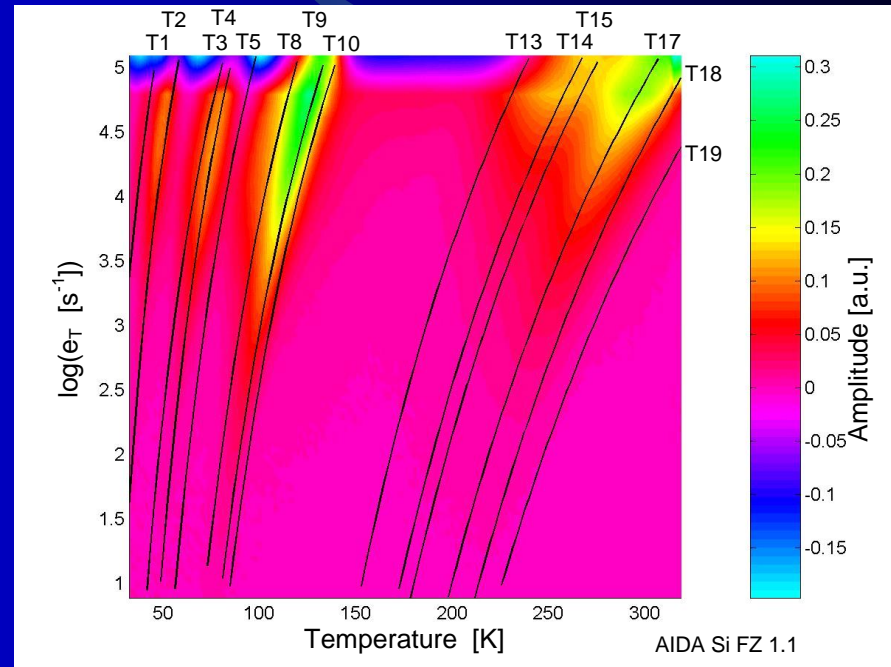
Images of two-dimensional spectra derived from the photocurrent relaxation waveforms by using the correlation procedure

$$\Phi = 1 \times 10^{14} n_{\text{eq}} / \text{cm}^2$$

$$[N] = 9.8 \times 10^{14} \text{ cm}^{-3}$$



$$[N] = 2.26 \times 10^{15} \text{ cm}^{-3}$$



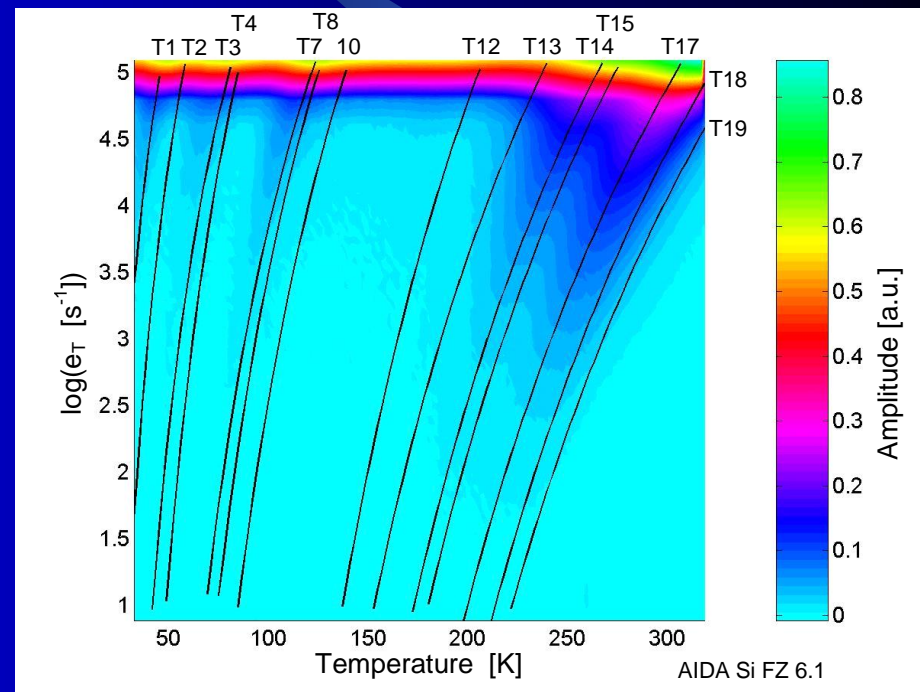
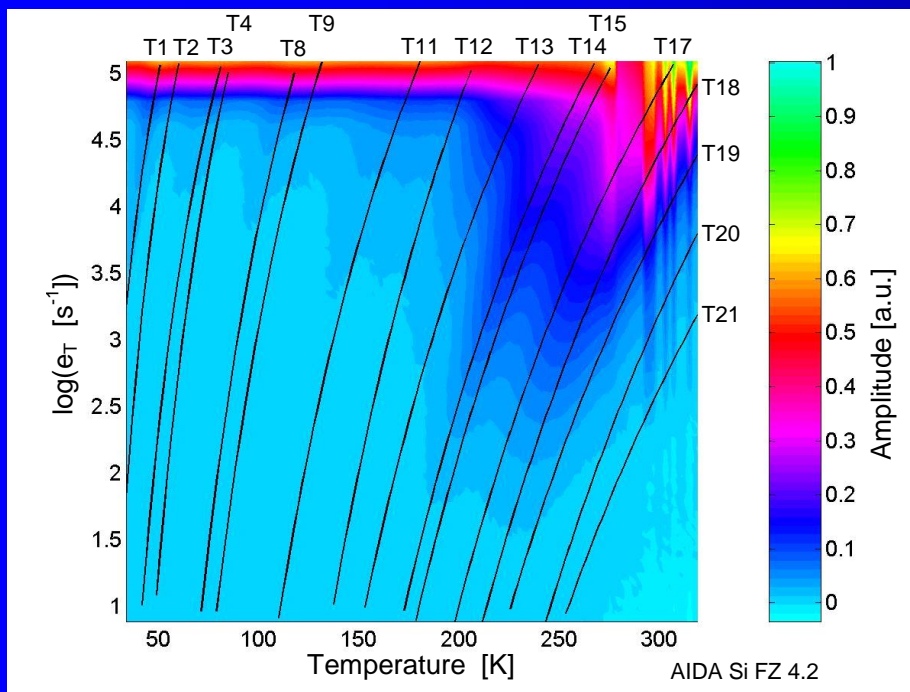
The solid lines illustrate the temperature dependences of thermal emission rate of charge carriers from detected defect centers according to Arrhenius formula:
 $e_T = AT^2 \exp(-E_a/kT)$.

Images of two-dimensional spectra derived from the photocurrent relaxation waveforms by using the correlation procedure

$$\Phi = 5 \times 10^{14} \text{ n}_{\text{eq}} / \text{cm}^2$$

$$[N] = 1.42 \times 10^{15} \text{ cm}^{-3}$$

$$[N] = 2.0 \times 10^{15} \text{ cm}^{-3}$$

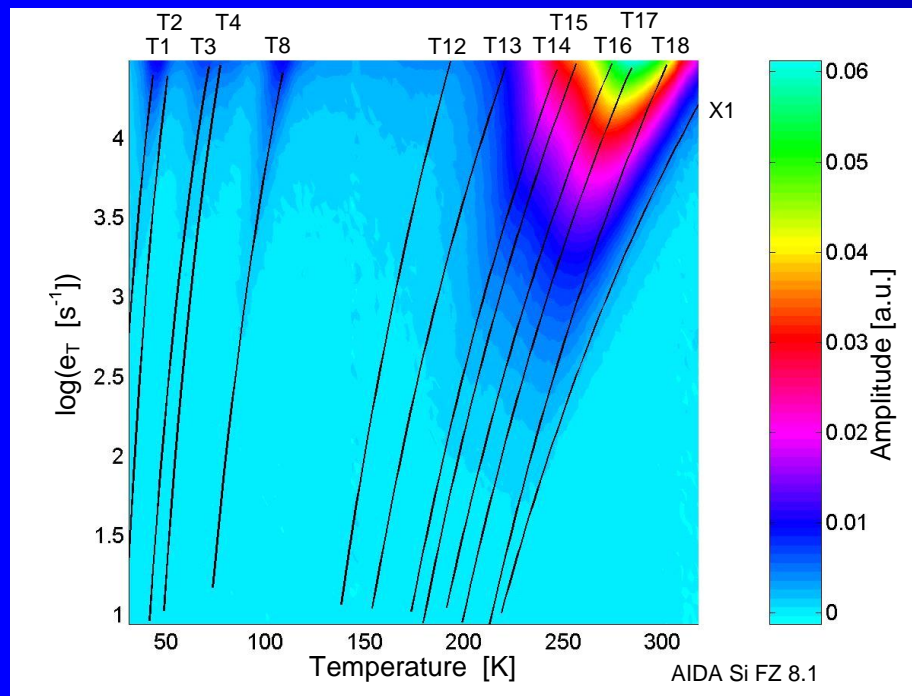


The solid lines illustrate the temperature dependences of thermal emission rate of charge carriers from detected defect centers according to Arrhenius formula:
 $e_T = AT^2 \exp(-E_a/kT)$.

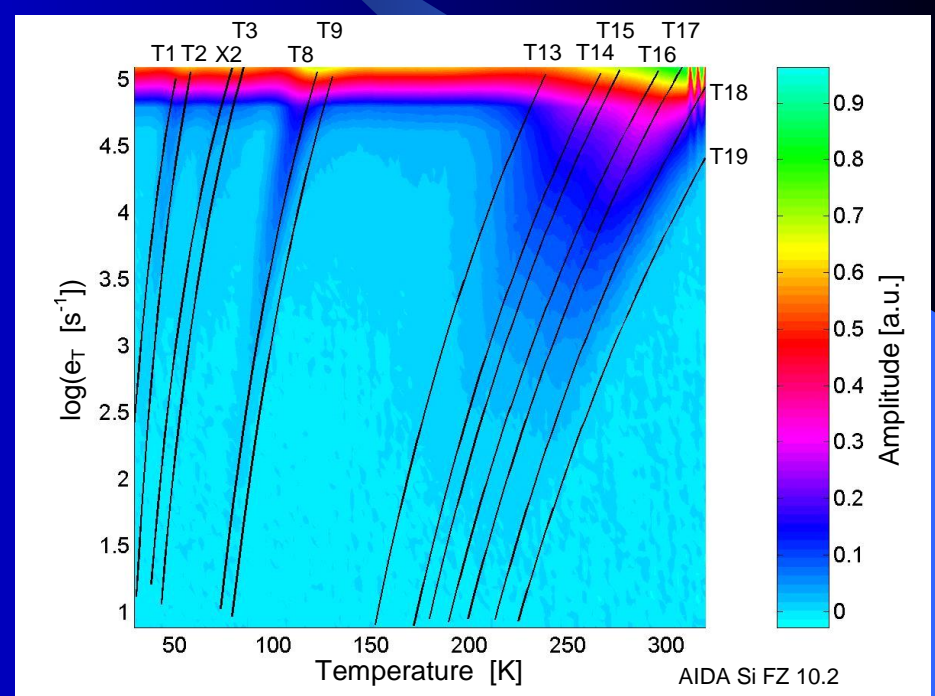
Images of two-dimensional spectra derived from the photocurrent relaxation waveforms by using the correlation procedure

$$\Phi = 1 \times 10^{15} \text{ n}_{\text{eq}}/\text{cm}^2$$

$$[N] = 9.2 \times 10^{14} \text{ cm}^{-3}$$



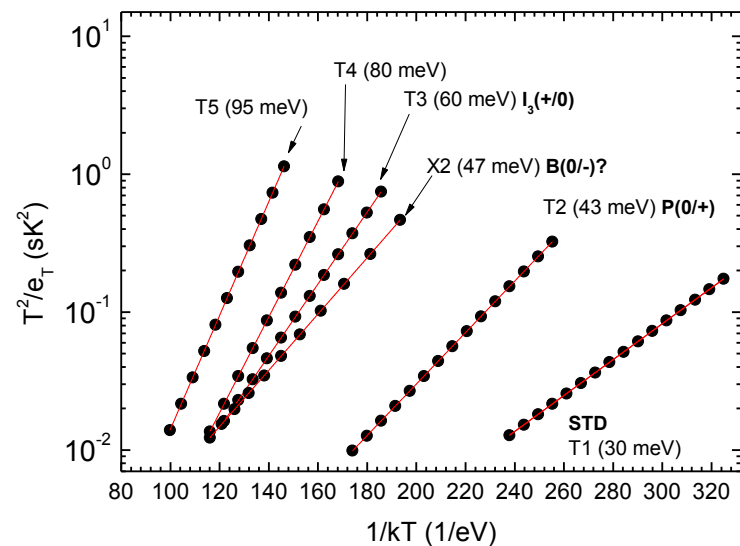
$$[N] = 2.5 \times 10^{15} \text{ cm}^{-3}$$



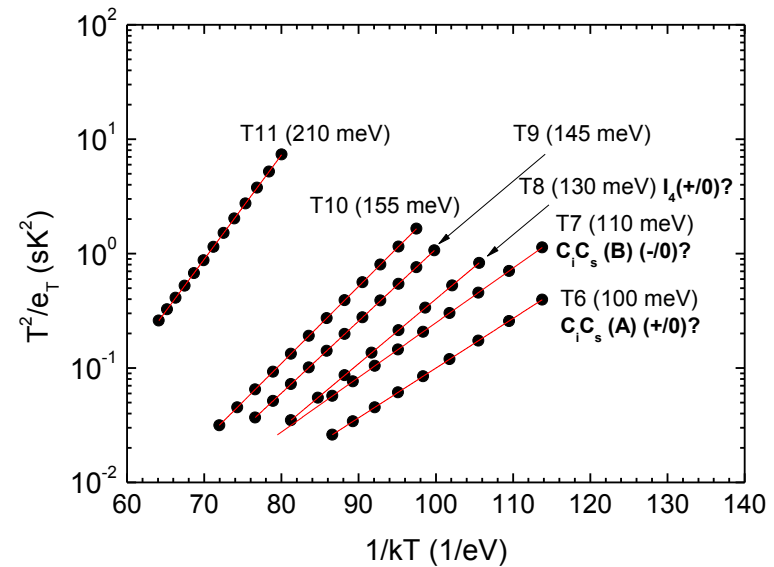
The solid lines illustrate the temperature dependences of thermal emission rate of charge carriers from detected defect centers according to Arrhenius formula: $e_T = AT^2 \exp(-E_a/kT)$.

Arrhenius plots for the resolved defect centers

Temperature range: 30 – 120 K

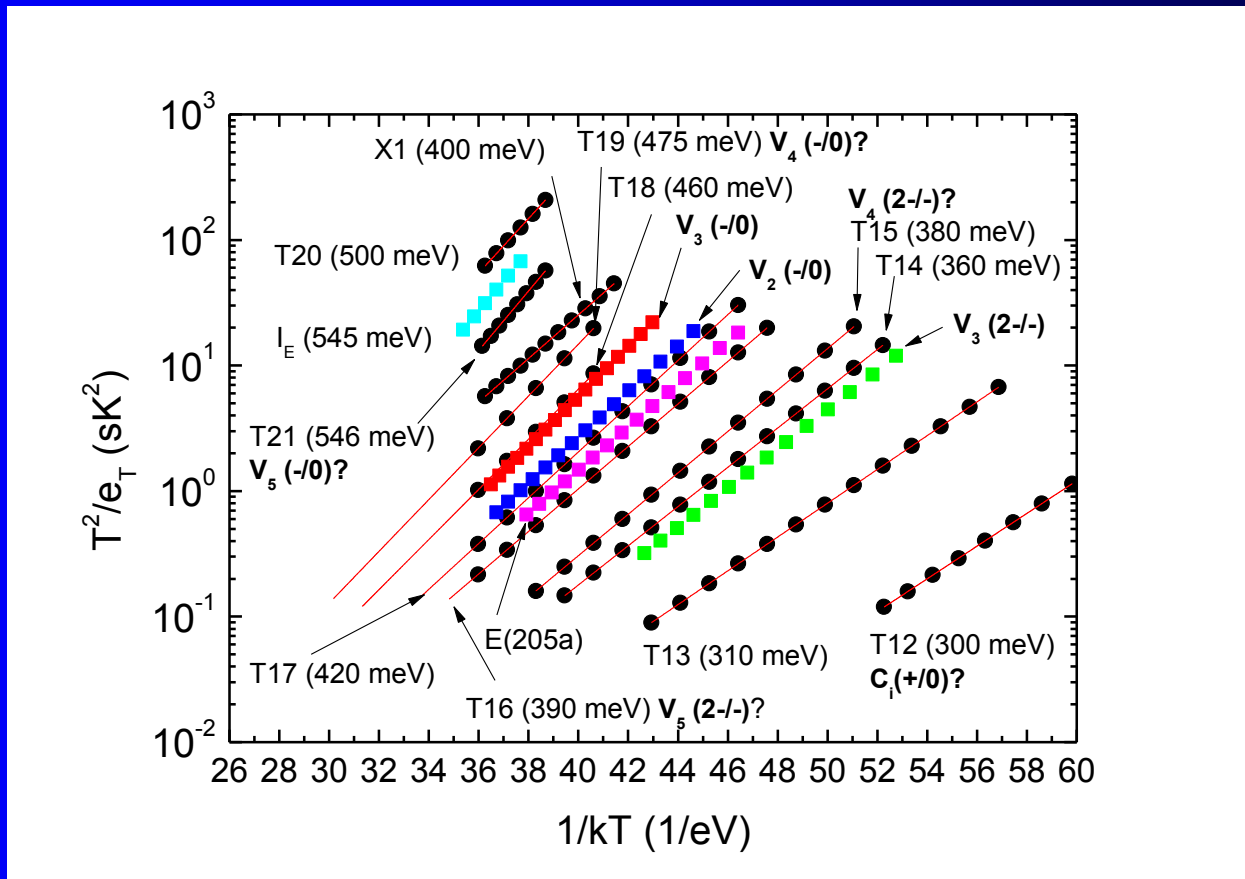


Temperature range: 100 – 180 K



Arrhenius plots for the resolved defect centers

Temperature range: 190 – 320 K



Properties and identification of radiation defect centers (1)

Trap Label	E_a (meV)	A ($\text{K}^{-2}\text{s}^{-2}$)	Sample Label	Φ (neq/cm ²)	Tentative Identification
T1	30 ± 3	$(9.8 \pm 0.9) \times 10^4$	A - F	1E14, 5E14, 1E15	e , shallow thermal donor, oxygen aggregate
T2	43 ± 3	$(1.8 \pm 0.2) \times 10^5$	A - F	1E14, 5E14, 1E15	e , phosphorus donor, P (0/+)
X2	47 ± 3	$(1.9 \pm 0.2) \times 10^4$	F	1E15	h , boron acceptor, B (0/-)
T3	60 ± 5	$(9.0 \pm 0.9) \times 10^4$	A - F	1E14, 5E14, 1E15	h , donor, I ₃ (+/0)
T4	80 ± 5	$(7.9 \pm 0.7) \times 10^5$	B, C, D, E	1E14, 5E14, 1E15	not identified
T5	95 ± 5	$(9.4 \pm 0.9) \times 10^5$	B	1E14	not identified
T6	100 ± 10	$(2.2 \pm 0.2) \times 10^5$	A	1E14	h , donor, C _i C _s (A) (+/0)
T7	110 ± 10	$(2.4 \pm 0.2) \times 10^5$	A, D	1E14, 5E14	e , acceptor, C _i C _s (B) (-/0)
T8	130 ± 10	$(1.1 \pm 0.1) \times 10^6$	A - F	1E14, 5E14, 1E15	h , donor, I ₄ (+/0)
T9	145 ± 10	$(2.1 \pm 0.3) \times 10^6$	B, C, F	1E14, 5E14, 1E15	not identified
T10	155 ± 10	$(2.2 \pm 0.2) \times 10^6$	B, D	1E14, 5E14	N-related ?
T11	210 ± 10	$(2.7 \pm 0.3) \times 10^6$	C	5E14	not identified
T12	300 ± 10	$(5.4 \pm 0.5) \times 10^7$	A, C, D, E	1E14, 5E14, 1E15	h , donor, C _i (+/0) ?

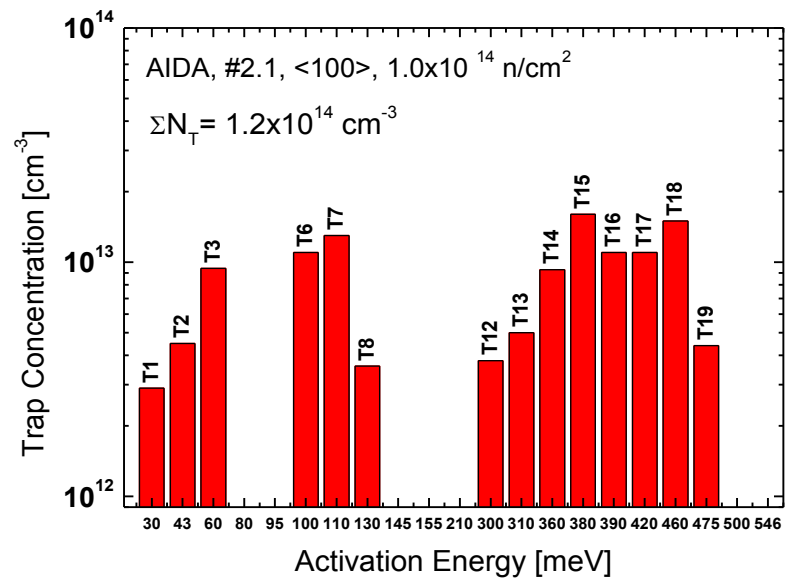
Properties and identification of radiation defect centers (2)

T13	310±10	$(6.7\pm0.6)\times10^6$	A - F	1E14, 5E14, 1E15	not identified
T14	360±15	$(1.0\pm0.1)\times10^7$	A - F	1E14, 5E14, 1E15	<i>e</i> , acceptor, V ₃ (2/-)
T15	380±15	$(1.3\pm0.1)\times10^7$	A - F	1E14, 5E14, 1E15	<i>e</i> , acceptor, V ₄ (2/-)
T16	390±15	$(5.7\pm0.5)\times10^6$	A, E, F	1E14, 5E14	<i>e</i> , acceptor, V ₅ (2/-)
X1	400±20	$(3.5\pm0.3)\times10^5$	E	1E15	not identified
T17	420±20	$(9.6\pm1.0)\times10^6$	A - F	1E14, 5E14, 1E15	<i>e</i> , acceptor, V ₂ (-/0)
T18	460±20	$(1.5\pm0.2)\times10^7$	A - F	1E14, 5E14, 1E15	<i>e</i> , acceptor, V ₃ (-/0)
T19	475±20	$(1.0\pm0.2)\times10^7$	A, B, C D, F	1E14, 5E14, 1E15	<i>e</i> , acceptor, V ₄ (-/0)
T20	500±20	$(1.2\pm0.2)\times10^7$	C	5E14	not identified
T21	546±20	$(2.6\pm0.3)\times10^7$	C	5E14	<i>e</i> , acceptor, V ₅ (-/0)

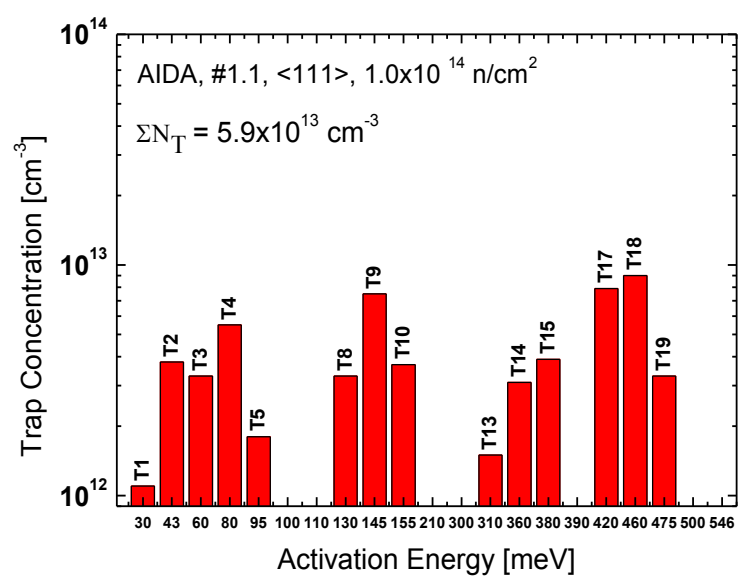
Concentrations of radiation defect centers

$$\Phi = 1 \times 10^{14} \text{ n}_{\text{eq}} / \text{cm}^2$$

Sample A, $[N] = 9.8 \times 10^{14} \text{ cm}^{-3}$



Sample B, $[N] = 2.26 \times 10^{14} \text{ cm}^{-3}$



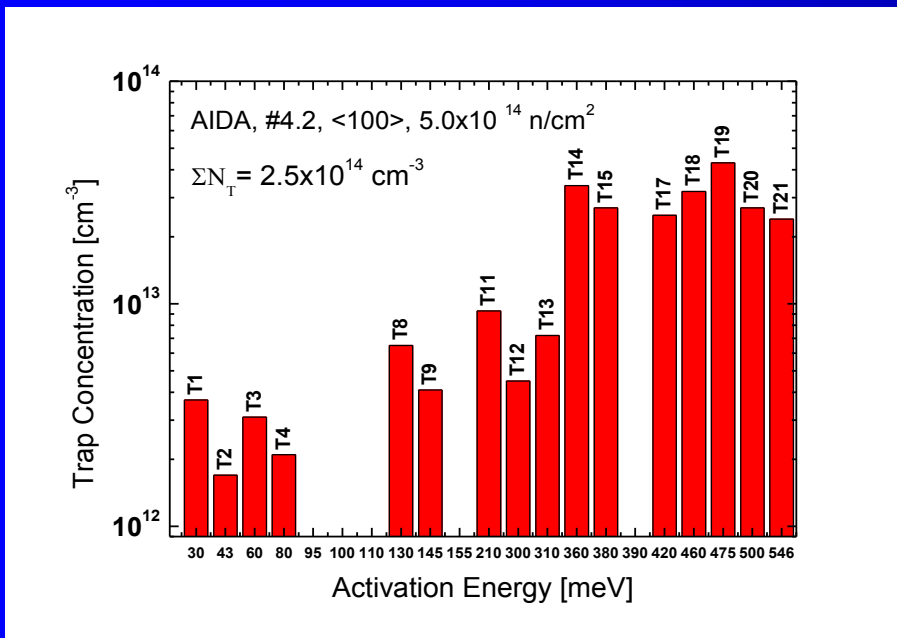
Total traps concentration: $1.2 \times 10^{14} \text{ cm}^{-3}$

Total traps concentration: $5.9 \times 10^{13} \text{ cm}^{-3}$

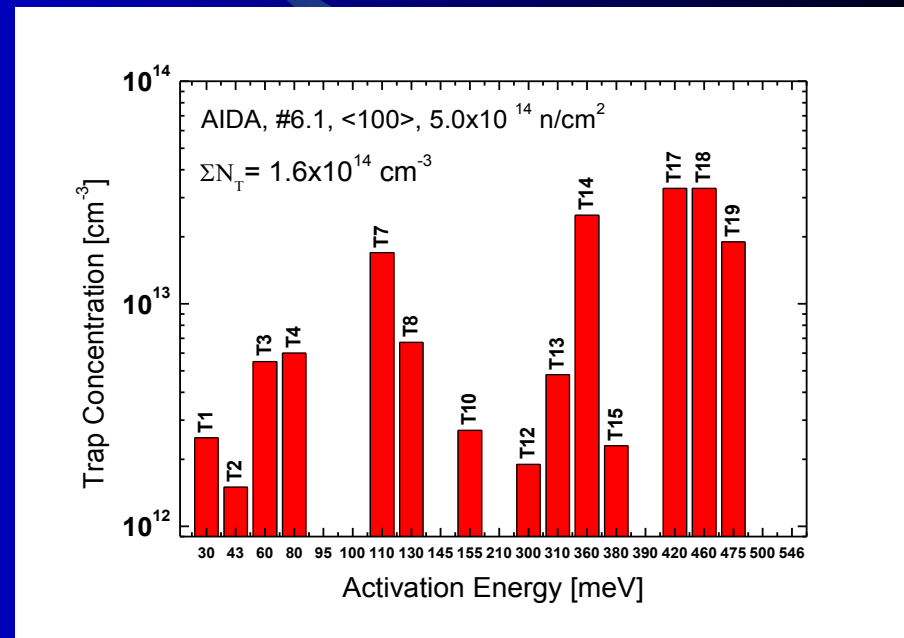
Concentrations of radiation defect centers

$$\Phi = 5 \times 10^{14} \text{ n}_{\text{eq}}/\text{cm}^2$$

Sample C, $[N] = 1.42 \times 10^{15} \text{ cm}^{-3}$



Sample D, $[N] = 2.0 \times 10^{15} \text{ cm}^{-3}$



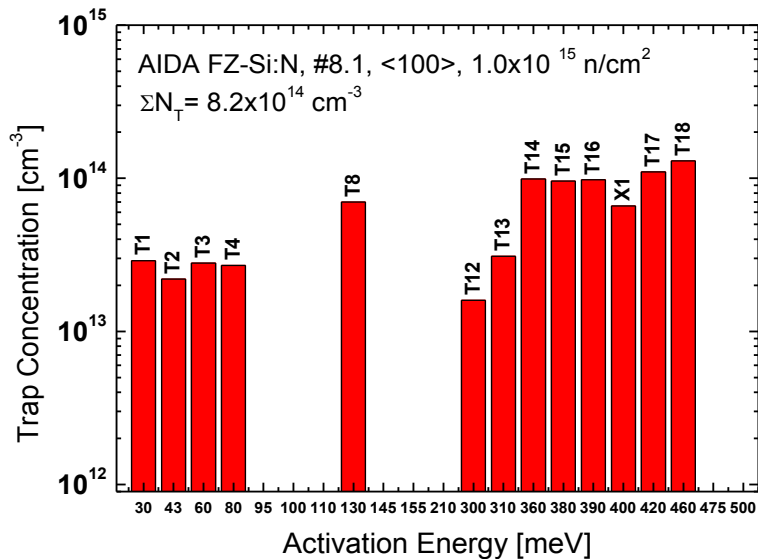
Total traps concentration: $2.5 \times 10^{14} \text{ cm}^{-3}$

Total traps concentration: $1.6 \times 10^{14} \text{ cm}^{-3}$

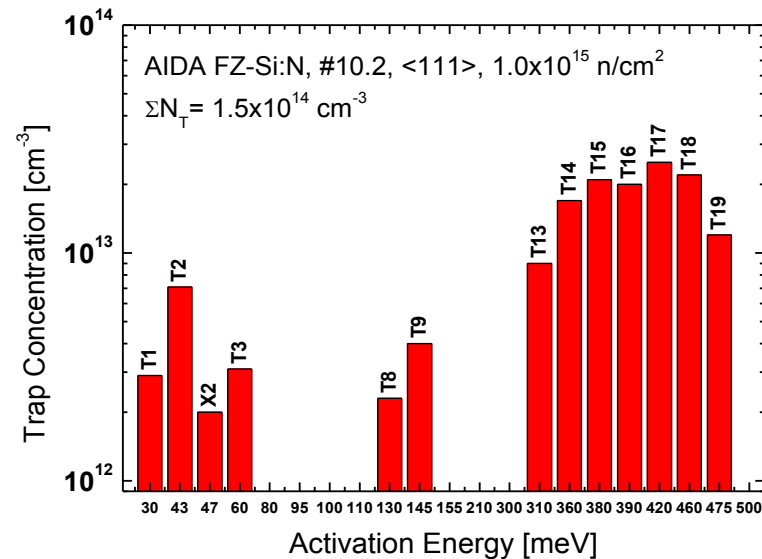
Concentrations of radiation defect centers

$$\Phi = 1 \times 10^{15} \text{ n}_{\text{eq}}/\text{cm}^2$$

Sample E, $[N] = 9.2 \times 10^{14} \text{ cm}^{-3}$



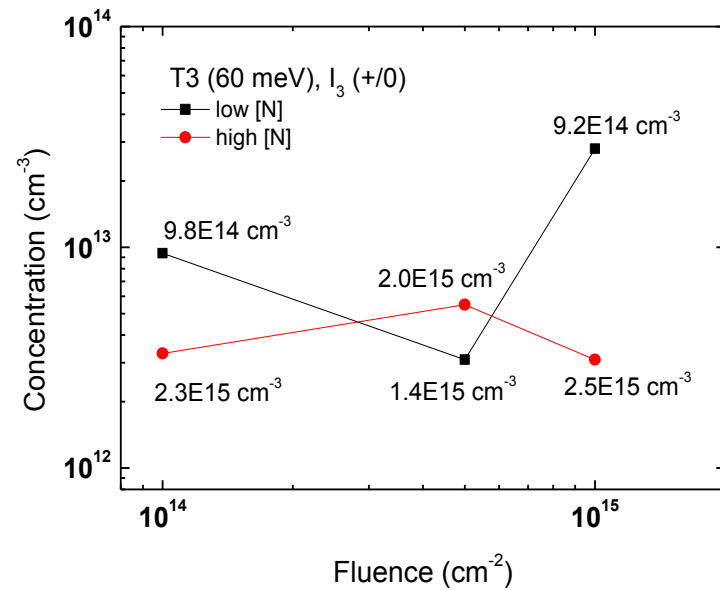
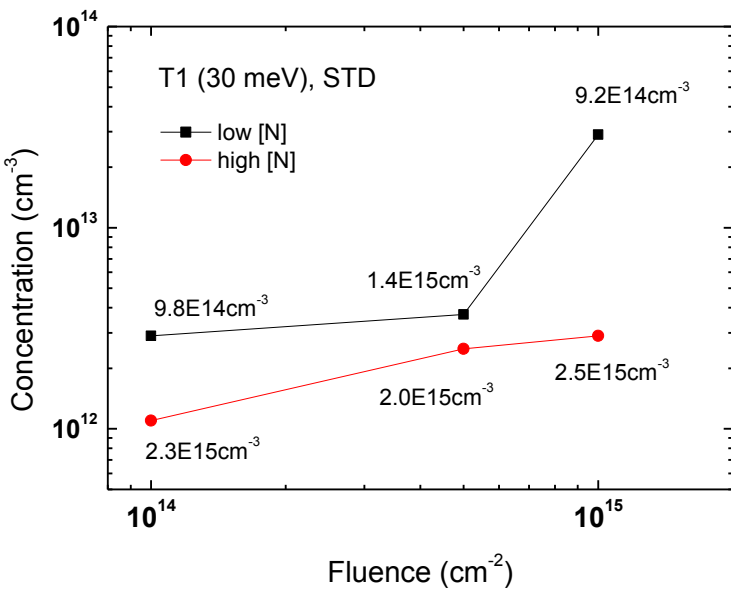
Sample F, $[N] = 2.50 \times 10^{14} \text{ cm}^{-3}$



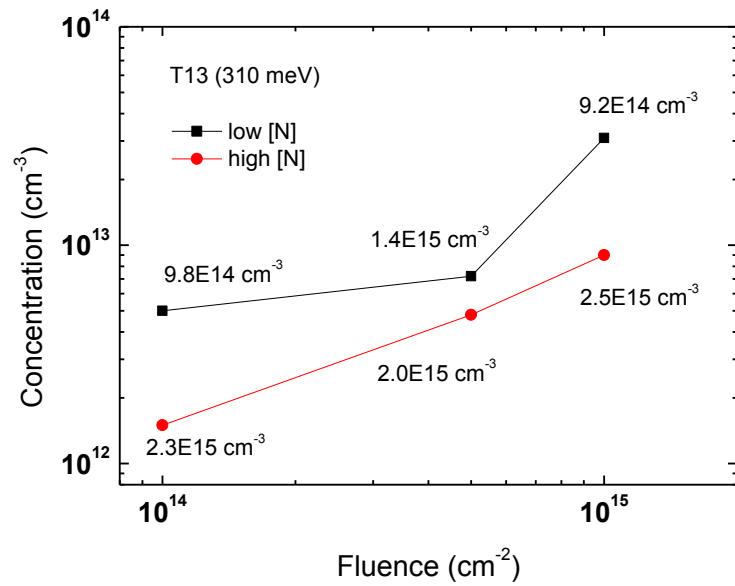
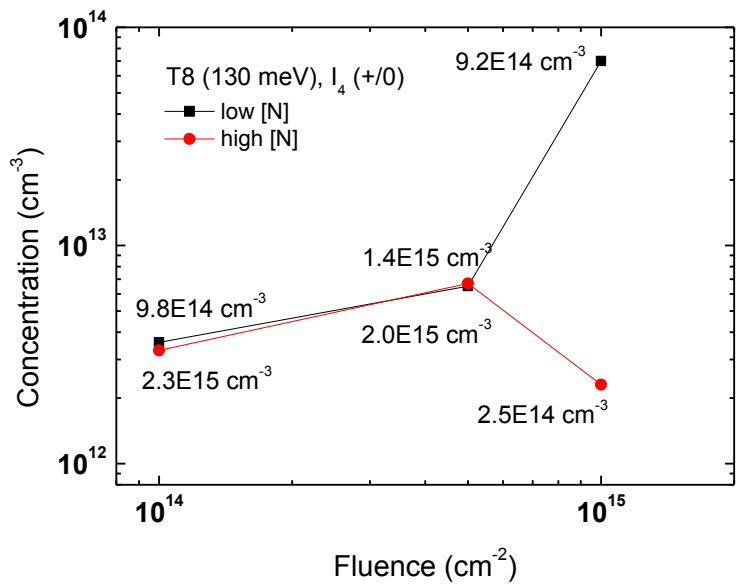
Total traps concentration: $8.2 \times 10^{14} \text{ cm}^{-3}$

Total traps concentration: $1.5 \times 10^{14} \text{ cm}^{-3}$

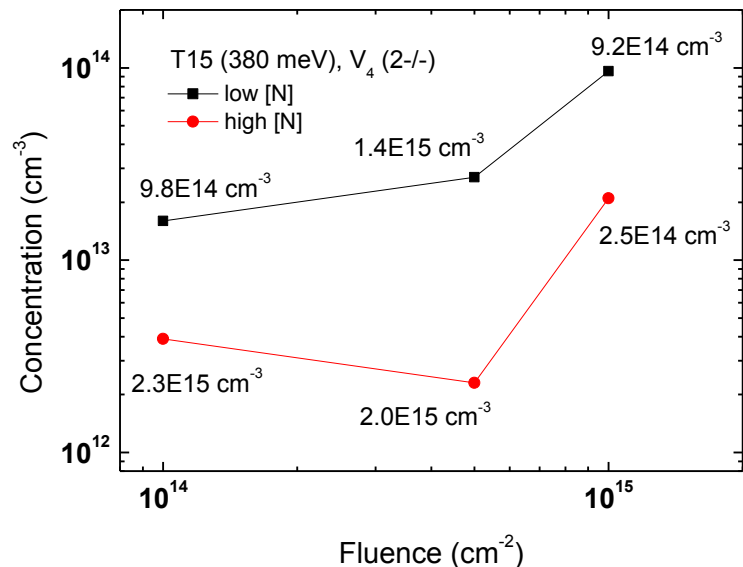
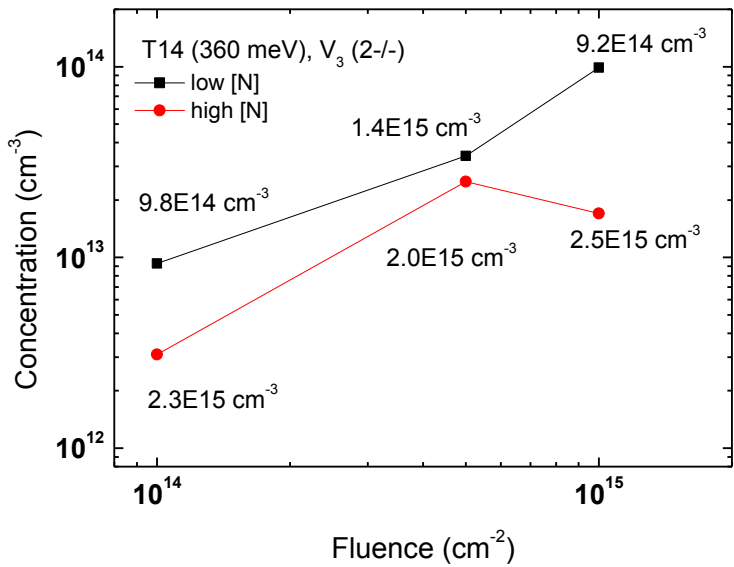
Nitrogen impact on concentrations of electrically active radiation defect centers



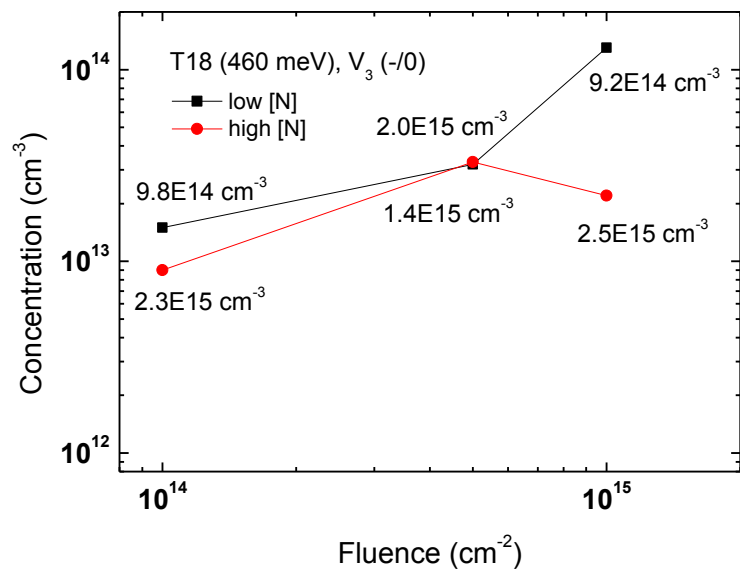
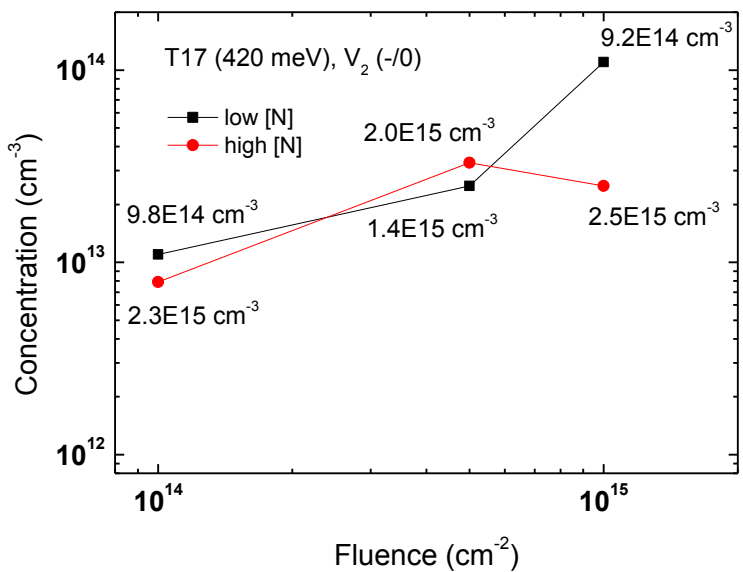
Nitrogen impact on concentrations of electrically active radiation defect centers



Nitrogen impact on concentrations of electrically active radiation defect centers



Nitrogen impact on concentrations of electrically active radiation defect centers



Conclusions

- We have demonstrated the effect of neutron fluence ranging from 10^{14} to $10^{15} \text{ n}_{\text{eq}}/\text{cm}^2$ on the properties and concentrations of electrically active radiation defect centers in N-doped, high-resistivity FZ Si.
- The defect structure of the irradiated material is found to be complex. More than 20 irradiation-induced defect centers with activation energies of 30 – 550 meV were detected. The main centers are likely to be attributed to shallow thermal donors, small interstitial clusters and small vacancy clusters in various charge states.
- The increase in the nitrogen concentration from $\sim 9 \times 10^{14}$ to $2.5 \times 10^{15} \text{ cm}^{-3}$ seems to result in diminishing the concentrations of some radiation defect centers, in particular of shallow thermal donors as well as small clusters of vacancies and interstitials.
- Further studies on the nitrogen impact on the properties and concentrations of radiation defect centers are in progress.

Acknowledgements

This work has been partially supported by the National Centre for Research and Development within the framework of the NitroSil project (ID: 208346) financed by the Program for Applied Research (Contract No. PBS2 / A9 / 26/2014). The neutron irradiations have received funding from the European Commission under the FP7 Research Infrastructures project AIDA by grant agreement No. 262025.

Thank you for your attention